

Article

Impact of Heat Treatment Conditions and Cold Plastic Deformation on Secondary Hardening and Performance of Cold Work Tool Steel X160CrMoV12

Regita Bendikiene * and Lina Kavaliauskiene

Department of Production Engineering, Faculty of Mechanical Engineering and Design, Kaunas University of Technology, Studentu St. 56, 51424 Kaunas, Lithuania; lina.kavaliauskiene@ktu.lt
*Correspondence: regita.bendikiene@ktu.lt; Tel.: +370-698-01202.

Abstract: In this study, the effect of the cold plastic deformation of a Bridgman anvil at room temperature on the hardness and wear resistance of X160CrMoV12 steel was investigated by utilizing the hardness test, X-ray diffraction (XRD), abrasive emery wear (AEMW) test, optical examination, and scanning electron microscopy (SEM). Three batches of samples were prepared for the experiment: I—as-hardened, II—after hardening with subsequent tempering at 600 °C for 1.5 h, and III—after hardening with subsequent plastic deformation. The hardening of the samples was performed at three temperatures: 1100 °C, 1150 °C, and 1200 °C. The highest content of retained austenite, as much as 69.02%, was observed during hardening at 1200 °C, while 17.36% and 38.14% were formed at lower temperatures, respectively. After tempering (Batch II), the content of residual austenite decreased proportionally by a factor of about seven for each hardening temperature. The effect of plastic deformation (Batch III) is observed, analyzing the hardness of the samples from the surface to the depth, reaching an average hardened depth of 0.08 mm. To evaluate the wear resistance, the surfaces of the three test batches were subjected to an abrasive emery wear test under a 5 N load. Hardened and plastically deformed samples showed higher wear resistance than hardened and tempered samples. The results confirmed that the optimal hardening temperature to achieve the maximum wear resistance of this steel is 1100 °C.

Citation: Bendikiene, R.; Kavaliauskiene, L. Impact of Heat Treatment Conditions and Cold Plastic Deformation on Secondary Hardening and Performance of Cold Work Tool Steel X160CrMoV12. *Metals* **2024**, *14*, 1121.

<https://doi.org/10.3390/met14101121>

Academic Editor: Daniela Pilone

Received: 4 September 2024

Revised: 27 September 2024

Accepted: 30 September 2024

Published: 1 October 2024



Copyright: © 2024 by the authors. Licensee MDPI, Basel, Switzerland. This article is an open access article distributed under the terms and conditions of the Creative Commons Attribution (CC BY) license (<https://creativecommons.org/licenses/by/4.0/>).

Keywords: cold work tool steel; retained austenite; tempering; secondary hardening; Bridgman anvil deformation; wear resistance

1. Introduction

High-carbon and high-chromium tool steels are important engineering materials for the production of cutting tools and cold forming dies. They are the main alloys of this group, with the largest number of alloying elements in cold-worked tool steels. Due to the resulting dense chromium carbides, which distinguish them from other alloys, they have high wear resistance and even corrosion resistance. This positive effect on the mechanical properties of tool steel is explained by the formation of two types of carbides, namely primary and secondary carbides [1]. Primary carbides increase resistance to abrasive wear, while secondary carbides affect resistance to plastic deformation [2]. Therefore, these steels can withstand high wear stress during service, especially when used for moulds and tools [3]. Due to its high chromium content, this steel is much more resistant to oxidation at high temperatures than plain carbon steel or other low-alloy steels. At the same time, this steel is usually subjected to compressive and tensile and shear stresses; therefore, cold-worked tool steel requires high strength and hardness, in addition to good wear resistance.

Generally, increasing the hardness of a material increases its wear resistance, but this correlation is only valid for pure annealed metals and alloys of the same family [4].

Therefore, in principle, all the research conducted is aimed at improving wear resistance, mainly by changing the microstructure using conditional heat treatment methods [5,6]. The required mechanical and performance properties are achieved by selecting the proper heat treatment routine, resulting in the formation of a specific microstructure. High hardness is often produced by the transformation of austenite to martensite, and toughness is mainly controlled by the tempering of martensite. The size and distribution of grains or phases in the tool steel microstructure can also be further modified by subsequent heat treatment or other processes [7,8]. As a result of conventional hardening, the martensitic matrix is reinforced with dispersed carbides, which leads to notable strength and hardness increments.

The retained austenite transformation in high-carbon and -chromium steel has long been a subject of scientific interest, but its characterization and understanding remain challenges [9,10]. The literature suggests that retained austenite can transform into ferrite and cementite, martensite, or bainite. Ferrite and cementite are formed during isothermal treatment at the tempering temperature, and the latter transformation occurs on cooling from the tempering temperature. The isothermal transformation to ferrite and carbide is shown to be a two-step process [11]. First, cementite is precipitated from retained austenite, which gradually transforms into ferrite and cementite. These observations were made for carbon, bainite, and hot work tool steels. Thus, the mechanism by which the retained austenite transforms depends on the composition of the steel and the heat treatment procedure and has a significant impact on the resulting mechanical properties [12]. Although the mechanism is known, there is a lack of information in the literature on the transformation of retained austenite during the tempering of cold work tool steel.

The wear resistance of this type of steel is attributed to the high volume fraction of hard chromium carbides and is about eight times that of plain carbon steel [3]. Abrasive wear loss decreases with increasing martensite volume fraction. A two-phase structure with a small amount of ferrite and a large amount of martensite provides better wear resistance than a fully martensitic microstructure [6]. It has been reported that under high-stress abrasive wear conditions, samples with a bainitic structure exhibit better wear resistance compared to tempered martensite samples with similar mechanical properties [13]. This occurs because the retained austenite in bainitic samples can increase the wear resistance as it transforms from retained austenite to martensite. Other authors focused on industrial wear research during the cold winding of cold-worked tool steel, combining the effects of wear and lubrication type on the evolution of the coefficient of friction during cold working, seeking to extend the lifespan of high-carbon and -chromium tool steels [14]. However, all these measures are not sufficient, especially in cases where parts and components operate under high wear and tear conditions. In such cases, after conventional heat treatment, the properties of metallic material surfaces can be modified by severe plastic deformation (SPD) [15,16], including uniform channel angular pressing, high-pressure torsion, accumulative roll bonding, scouring (SP), surface mechanical abrasive treatment (SMAT), and friction stir processing (FSP) [3,15–19]. Almost any type of material can be subjected to extremely high stresses using the high-pressure torsion method. Continuous shear stress and high compressive stresses are useful for grain refining [18], which afterwards directly affects wear resistance. Since the deformation takes place at room temperature, thermal damage to the materials is avoided and their properties are preserved, and the mechanical and functional properties of the final material variant are significantly improved due to large deformations. In addition, a very complex microstructure with a very high concentration of lattice defects is obtained, and colonies of micro- and nano-grains are formed.

Cold plastic deformation, such as cold rolling, can significantly impact the mechanical properties of high-alloy steels like X160CrMoV12. For instance, cold rolling of high-alloyed TRIP steel can lead to a high amount of α' -martensite and result in an ultrafine-grained reverted austenitic microstructure with a mean grain size of about 1 μm . This process can lead to an enormous increase in yield strength of up to 1000 MPa [20].

Additionally, accumulative roll bonding (ARB) of high-alloy steels can enhance their mechanical properties, with steel laminates exhibiting superior properties among laminated metal composites. The deformation mechanisms of twinning- and transformation-induced plasticity (TWIP and TRIP) in high-alloy steels are crucial for understanding their mechanical behaviour [21]. Cold plastic deformation plays a vital role in improving the mechanical properties of high-alloy steels like X160CrMoV12, leading to increased strength and unique microstructures that contribute to the longer life and higher performance of critical industrial components.

This paper examines the behaviour of sX160CrMoV12 steel during the heat treatment process, comparing the conventional operations, i.e., hardening with subsequent tempering, and the influence of less traditional plastic deformation on wear resistance. The cold work die steel X160CrMoV12 is used in the metalworking industry to produce castings, rollers, die plates and dies, eyes for the calibration of metal, dies and punches for blanking dies, and punches and dies for cold extrusion, operating with working pressures up to 1400–1600 MPa. To explore the possibilities of this steel, higher-than-usual hardening temperatures were chosen. The high temperature ensured the formation of a relatively large amount of residual austenite, the transformation of which later provided additional mechanical characteristics such as wear resistance. These results are not only useful from a scientific point of view, but they are also important for the metalworking industry, as they provide useful, practically and experimentally verified insights into the specifics of cold work tool steel X160CrMoV12 processing technology.

2. Materials and Methods

The steel chosen for the tests, X160CrMoV12, contains between 11 and 12.5% Cr (Table 1), which increases the hardenability of the steel: it promotes the dissolution of special carbides during tempering, and at the same time increases the steel's secondary hardness (increase in hardness by tempering the hardened steel) and heat resistance, and also increases the number of chromium carbides, which increases the wear resistance of the steel [22–24].

Table 1. Chemical composition of X160CrMoV12*.

Elements	Fe	C	Cr	Mo	V	Si	Mn
wt.%	Balance	1.45–1.65	11.0–12.5	0.4–0.6	0.15–0.30	0.1–0.5	0.15–0.45

* AFNOR NF A35-590(1992)

The steel for this study was forged, soft-annealed, and supplied as 13 mm bars from the same heat. Samples with dimensions of 10 × 10 × 50 mm³ were prepared for heat treatment (hardening with subsequent tempering), plastic deformation, microstructure analysis, and further wear resistance tests according to the experimental setup.

Heat treatment processes were accomplished in the laboratory muffle furnace N 7/H (Nabertherm GmbH, Lilienthal, Germany) with integrated time and temperature controls. Three hardening temperatures were chosen for the operation: 1100 °C, 1150 °C, and 1200 °C. After hardening, all samples were cooled in agitated oil. Batch I was subjected to the following tests in an as-hardened condition. Batch II samples were tempered at 600 °C, held for 1.5 h, and air-cooled. Batch III samples were subjected to cold plastic deformation using a Bridgman anvil (Figure 1) at room temperature. This method allowed samples to experience up to 30% torsional strain while maintaining material integrity under high quasi-hydrostatic pressure. The high pressure (6 GPa) helped avoid the failure of the sample during the process, which is often a concern for large plastic deformations. Initially, samples with a thickness of 10 ± 0.02 mm were rotationally deformed. They were placed between two hard metal anvils, each 50 mm in diameter, and rotated at approximately 1 rpm speed. The combination of rotational motion and applied pressure effectively deformed the samples, resulting in a significant reduction in thickness. After deformation,

the thickness of the samples was reduced by 30%, resulting in approximately 7 mm thick specimens with a diameter of 50 mm. This decrease in thickness indicates that the Bridgman anvil induces high plastic strain. Deformation was quantified by measuring the volume change in the samples after processing, which is a common method for estimating the extent of plastic deformation [15]. This experimental method allowed significant deformation of the material without causing cracks or defects, which is very important for studying the mechanical behaviour of high-strength steels and alloys under extreme conditions. Using this method, the high hydrostatic pressure ensures more uniform deformation and suppresses failure modes such as cracking, making it ideal for creating refined microstructures in materials such as X160CrMoV12 steel.

Rockwell hardness (HRC) was measured to characterize the mechanical properties of the samples before and after the heat treatment, plastic deformation, and wear test. Hardness testing was performed on a Mitutoyo hardness testing device HM-200 (Mitutoyo Corporation, Kanagawa, Japan) with a diamond indenter with a dwell time of 10 s; Table 2 shows the average value of five measurements. The Vickers hardness (HV) of the plastically deformed samples was assessed to check hardness depth towards the base metal. Hardness values were recorded on the same Mitutoyo device in the direction perpendicular to the sample surface with a diamond indenter under a load of 0.98 N and a dwell time of 10 s.

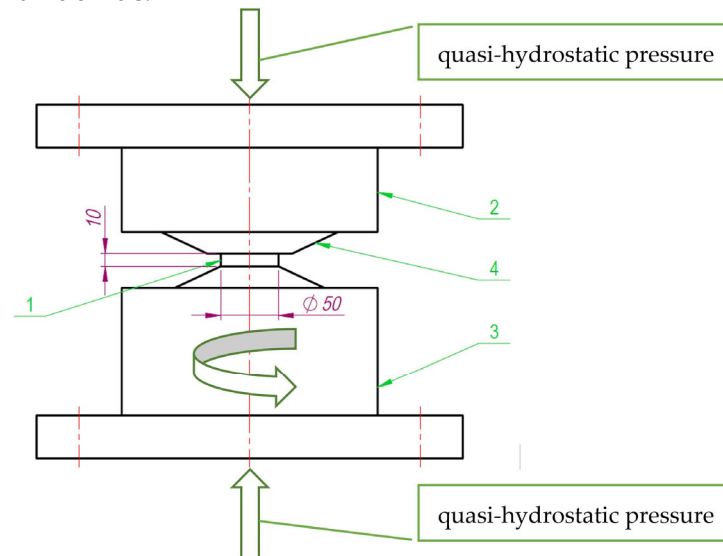


Figure 1. Schematic illustration of Bridgman anvil test: 1—sample; 2—fixed anvil; 3—movable anvil; 4—hard metal inserts.

Metallographic samples were prepared according to standard procedures, followed by etching with Nital 5% (95 ml methanol, 5 ml nitric acid). An optical micro analysis of the as-hardened samples at the indicated temperatures was performed using an MLA 10 and Carl Zeiss Axio Scope A1 (Carl Zeiss Spectroscopy GmbH, Jena, Germany). The microstructural images of samples after subsequent processing (tempering or plastic deformation) were analyzed using an (SEM) EVO MA-15 (Carl Zeiss AG, Oberkochen, Germany) scanning electron microscope, equipped with an energy-dispersive spectroscopy (EDS) device. The presence of retained austenite and types of precipitated carbides were estimated using the X-ray diffraction (XRD) device AXS D5005 (Bruker, Leipzig, Germany), equipped with a Cu K α radiation source.

The wear resistance of the samples was evaluated using the mass loss under abrasive emery wear (AEMW) (Figure 2) test conditions [25]. Samples with dimensions of 10 × 10 × 50 mm were prepared and tested for wear when the rotational speed around the holder axis was 0.4 m/s, the duration of the test was 60 min with intervals of 10 min each for the

replacement of the abrasive (electrocorundum/white aluminum oxide 15A8HM; mesh size F8). Mass loss was analyzed at every 10 min of the test (~ 240 m of wear path) on the laboratory scales with 0.001 g accuracy. The total length of the wear path was 2400 m.

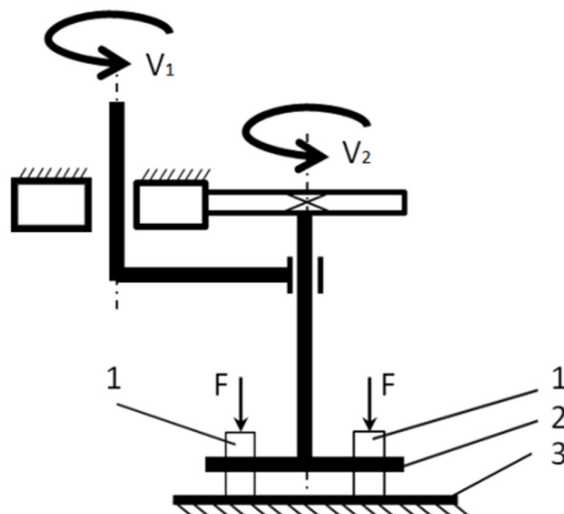


Figure 2. Principal scheme of abrasive emery wear test: 1—samples; 2—holder; 3—emery substrate.

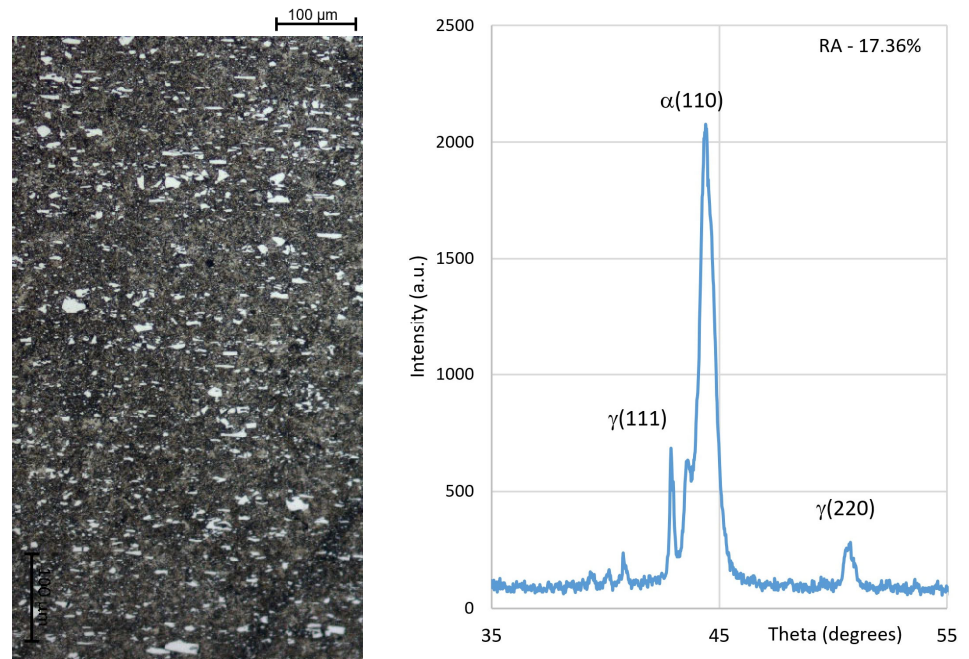
3. Results and Discussion

The X160CrMoV12 steel used in this study was supplied in an as-annealed condition. Among the promising properties of this alloy listed above, when the chromium content is increased to more than 4–5%, the chromium carbides in the workpiece are unevenly distributed: the carbides are arranged in "rows" and especially in the form of a "net", which greatly deteriorates the mechanical properties of the steel. This defect is most pronounced in high-chromium cold-worked die steels containing 6 to 12% chromium, which is the subject of this research work. This carbide non-uniformity can be reduced by the plastic deformation of the workpiece [15]. After the heat treatment of this steel, due to the presence of more than 1% carbon, it is expected to achieve sufficiently high hardness and, at the same time, relatively high wear resistance. This tool steel tends to form carbides due to its high content of carbide-forming elements. To achieve this, the heat treatment guide standard practice recommends hardening at around 1020–1050 °C (61–65 HRC) to obtain more retained austenite, which increases wear resistance [7,8,26]. In this study, it was decided to use slightly higher temperatures for hardening, as such a temperature range has not been studied in detail by other authors. When increasing the hardening temperature, the solubility of chromium carbides significantly increases, which boosts the content of chromium and carbon in austenite, and lowers the temperature of the beginning of the martensitic transformation, which facilitates the preservation of austenite after hardening. Only a relatively small amount of martensite is formed, while the austenite grain grows. The amount of extremely fine carbide phase is reduced. Therefore, a secondary hardening effect occurs after tempering. Samples of all batches, 45 in total, were subjected to the hardening process at 1100 °C, 1150 °C, and 1200 °C, followed by cooling in agitated oil. The selection of the tempering temperatures of 1100 °C, 1150 °C, and 1200 °C is based on the specific requirements for X160CrMoV12 steel. Temperatures from 1100 °C to 1200 °C allow the effects of increased retained austenite, carbide dissolution, and microstructure refinement to be controlled. The use of higher-than-standardized temperatures ensures that the mechanical properties of the steel can be adapted to demanding applications, improving wear resistance, toughness, and performance under difficult conditions. Five samples were used to study the hardening temperature of each batch, and the averages of the results were tabulated (Table 2) and used for comparison.

The hardness results tend to decrease from a maximum value of 61 HRC to a minimum of 35 HRC as the hardening temperature increases from 1100 °C to 1200 °C (Table 2). The hardness of this type of steel increases strongly in the hardening temperatures between 1000 °C and 1025 °C due to the higher concentration of alloying elements, but at higher process temperatures, which are the subject of this study, the hardness decreases, which is a consequence of the increased volume fraction of retained austenite [27]. The result of the decrease in hardness is confirmed by the optical analysis of the hardened samples. The microstructure, in general, consists of martensite (grey area, fine needles), retained austenite (light areas), and undissolved primary irregular spheroidal shape chrome carbides of M_7C_3 type (Figure 3). Even without determining the content of the retained austenite, a higher content is clearly visible in the sample hardened at 1200 °C.

Table 2. Hardness results after conventional hardening and further processing.

Batch	Hardening Temperature, °C	Hardness, HRC	Subsequent Treatment	Hardness after Subsequent Treatment, HRC
I	1100	61	None	61
	1150	55		55
	1200	35		35
II	1100	61	Tempered at 600°C for 1.5 h	47
	1150	55		49
	1200	35		51
III	1100	61	Plastic deformation, 30%	64
	1150	55		59
	1200	35		53



(a)

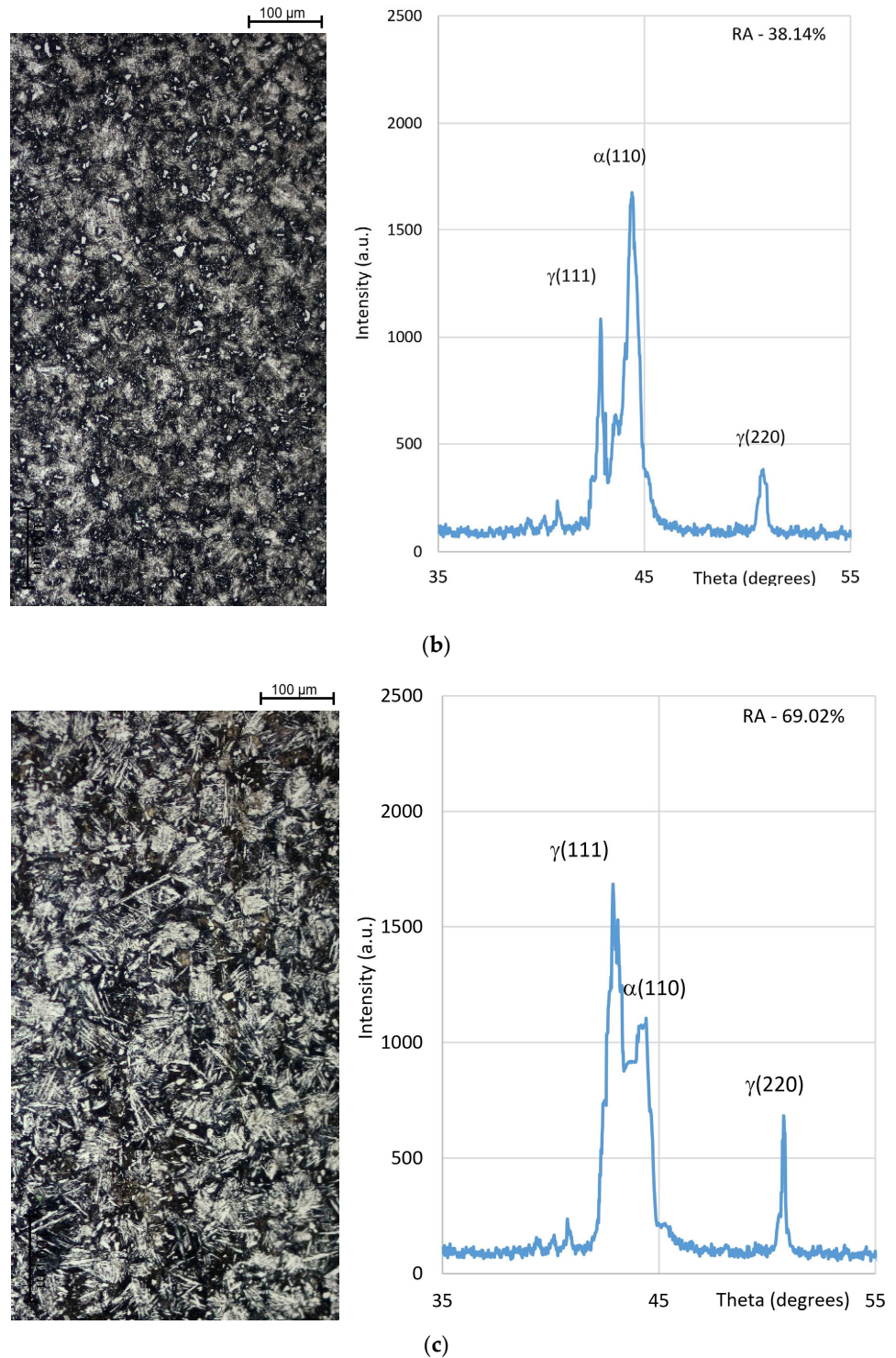
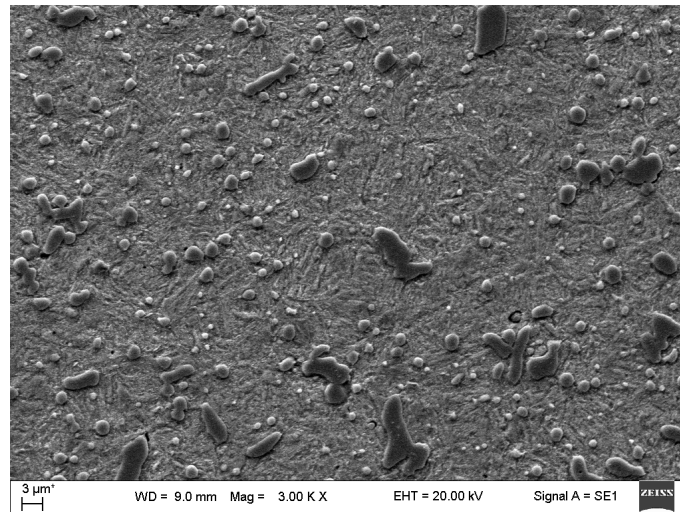


Figure 3. Microstructures and X-ray diffraction patterns of as-hardened samples at (a) 1100 °C; (b) 1150 °C; and (c) 1200 °C.

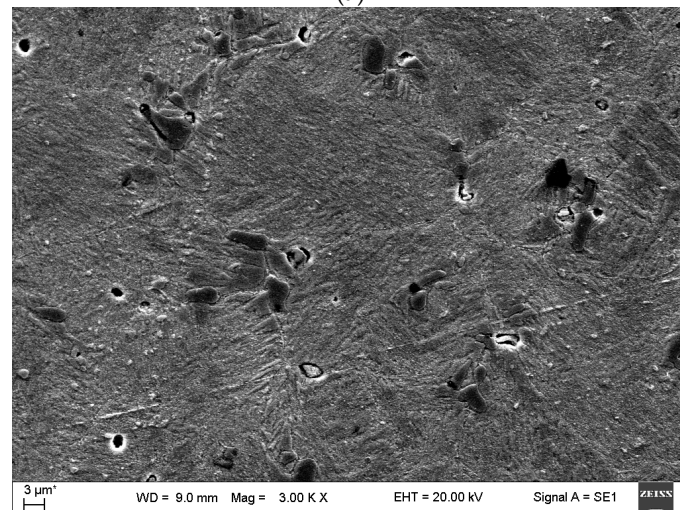
For high-chromium steels with a chromium-to-carbon ratio greater than 3, carbide transformations occur according to the following scheme: $M \rightarrow Fe_3C \rightarrow (Fe, Cr)_3C \rightarrow (Cr, Fe)_7C_3$ [7,28]. Primary chromium carbides (M_7C_3) rich in Fe [4] and arranged in lines in the microstructure of the sample hardened at 1100 °C (Figure 3a). Coarse-grained carbides

that do not dissolve during hardening inhibit austenite grain growth and are largely responsible for the high wear resistance. The linear distribution of carbides was not observed when the hardening temperature was increased to 1150 and 1200 °C (Figure 3b,c)—the higher the hardening temperature, the more uniform the distribution of the carbide phase in the matrix. The XRD graphs show peaks corresponding to two Theta degrees with angles of 42.88° and 50.76° which are assigned to the $\gamma(111)$ and $\gamma(220)$ planes, and 44.45°— $\alpha(110)$, which is the martensitic phase. The volume fraction of retained austenite increases on increasing the hardening temperature and ranges from 17.36% while hardened at 1100 °C to an intermediate value of 38.14% at 1150 °C and a maximum of 69.02% at 1200 °C. The clearly expressed change in the retained austenite volume fraction of about 24% is related to the increase in dissolved carbides at higher solidification temperatures [27,29].

After the previously described hardening procedure, the samples of Batch II were tempered at a temperature of 600 °C for 1.5 h and cooled in air. The microstructure of the sample tempered after hardening at 1100 °C shows a significant amount of secondary fine spheroidal carbides, which usually form at higher tempering temperatures [9], alongside a lower amount of primary irregular chrome carbides in the base of the fine martensite phase (Figure 4a).



(a)



(b)

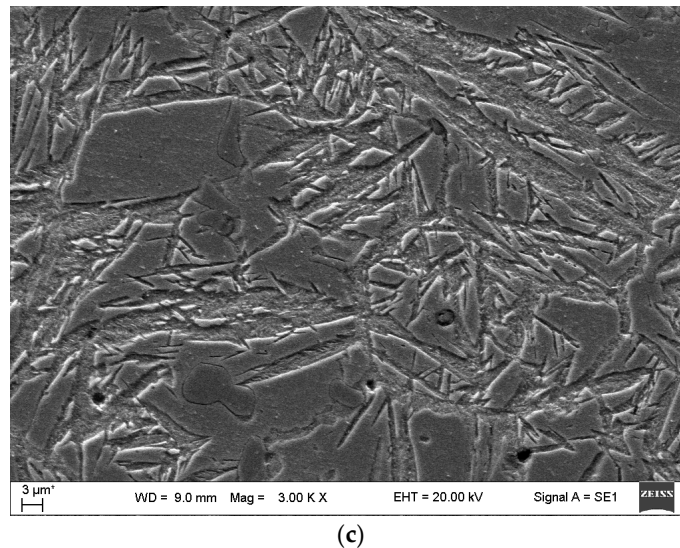


Figure 4. SEM micrographs of Batch II samples tempered at 600 °C for 1.5 h: (a) as hardened at 1100 °C; (b) as hardened at 1150 °C; (c) as hardened at 1200 °C.

Tempered martensite, carbides trapped in the matrix, and bainite plates with a relatively high remaining amount of retained austenite can be seen in Figure 4c. The sufficiently high amount of retained austenite in the as-hardened sample (RA 69.02%) was noticeably reduced. However, a single tempering cycle at 600 °C was not sufficient to completely transform the retained austenite in this sample. In order to completely free the retained austenite to a value of almost zero and receive the highest hardness for this type of steel, 62–64 HRC, and maximal toughness, double or even triple tempering is suggested [9,30]. However, in this study, it was decided to limit it to single tempering and to investigate how the samples from all three batches behaved under abrasive wear conditions.

The result of the retained austenite quantification in hardened and tempered samples (Figure 5) shows a visible decrease in RA volume fraction from 17.36% to 1.93% at the 1100 °C hardening temperature, from 38.14% to 7.26% at 1150 °C, and from 69.02% to 11.43% at 1200 °C. The secondary hardening effect after single tempering at a 600 °C temperature is not fully achieved, because the maximum obtained hardness does not exceed 60 HRC (Figure 5) for the sample hardened at the highest temperature (1200 °C). It is likely that the 11.43% volume fraction of retained austenite fully transforming into martensite after the second tempering would increase the hardness to the maximum value [31]. Based on the hardness values, it can be seen that the alloy carbides begin to dissolve, and the alloying elements enter the austenite phase. The austenite then cools to form a hard, supersaturated solid martensite. The alloying elements improve the stability of supercooled austenite and prevent carbide formation precipitation. Therefore, the structure contains retained austenite, undissolved carbides, and martensite while maintaining the austenite grain morphology [28].

Lower retained austenite volume fractions are observed at the tempering temperatures of 1100 °C and 1150 °C: 1.93% and 7.26%, respectively. A steady increase in carbide content is reported at lower tempering temperatures, with a sharper increase in the temperature range close to 600 °C [7]. Since this study considers only one tempering temperature, changes in carbide phase content are observed at different hardening temperatures, showing slight decreases in carbide content from 11.73% to 9.53% and 6.64% at 1100 °C, 1150 °C, and 1200 °C, respectively (Figure 5). The point of increase in the amount of retained austenite along with the decrease in the content of the carbide phase depends on the increase in the conventional hardening temperature [5]. According to the findings of other researchers [32], the presence of retained austenite significantly reduces the rate of

crack propagation, which can affect wear behaviour, and inhibits crack propagation at high stresses.

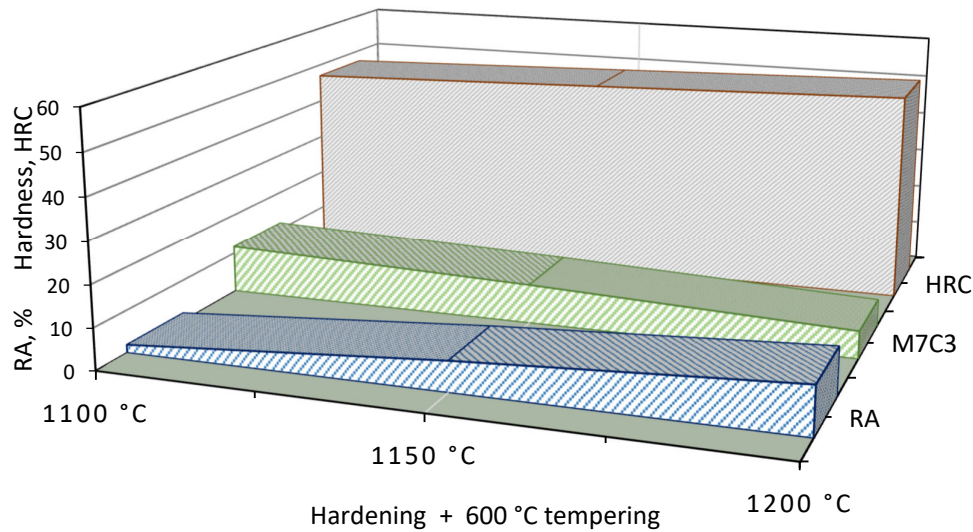


Figure 5. Content of retained austenite and carbide phase in the samples of Batch II after hardening at the indicated temperatures following by tempering at 600 °C.

Batch III samples were subjected to 30% plastic deformation in a torsional Bridgman anvil test after conventional hardening at different temperatures. It is known that large amounts of plastic deformation can have a significant effect on refining the grain sizes of materials [16,18], so it was decided to observe how the consequences of plastic deformation affected the wear resistance of the samples. The prepared samples were rotated under tension between two anvils under high pressure. The effect of plastic deformation was checked according to two criteria—the change in the microstructure of the surface layer (Figure 6) and the hardness values.

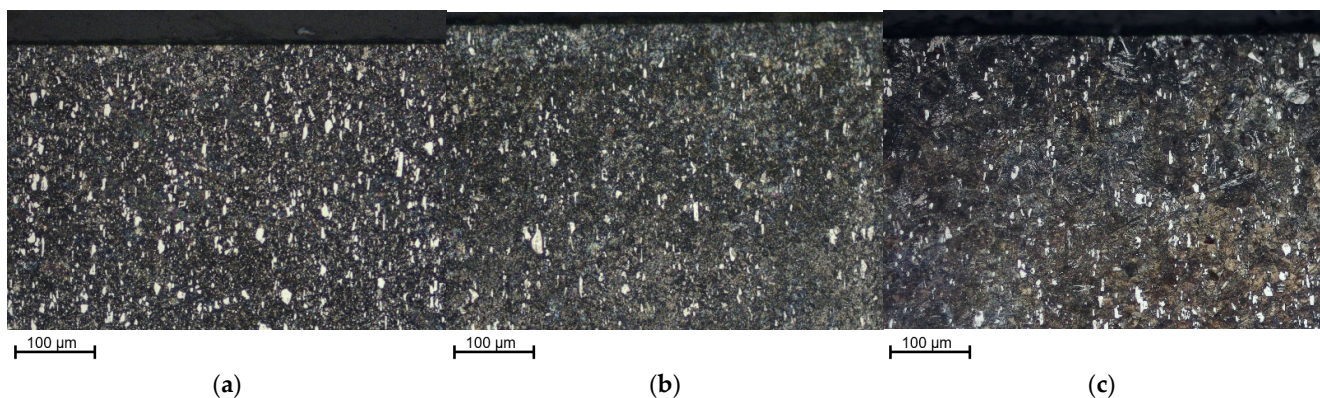


Figure 6. Optical microstructure images of plastically deformed samples after hardening at (a) 1100 °C; (b) 1150 °C; and (c) 1200 °C.

The average thickness of the plastically deformed layer of all samples was about 0.08 mm. In the microstructures, a significantly more uniform and finer structure is observed (Figure 6), which is different from the one we observed immediately after hardening (Figure 3). The Rockwell hardness values increased in proportion to those achieved by conventional hardening, showing the highest hardness peak achieved for this type of steel to be 64 HRC when hardened at 1100 °C, a slight increase (from 55 HRC to 59 HRC) at 1150

°C, and with the highest change at the maximum hardening temperature of 1200 °C, when the hardness value increased from 35 HRC to 53 HRC (Figure 7). The Vickers hardness HV_{0.1} test of the plastically deformed samples confirmed the assumption that the surface layer hardens and then gradually decreases as it moves towards the centre of the sample until reaching base metal hardness (Figure 8). The hardness of the samples hardened at 1100°C changed from 840 HV_{0.1} (~64 HRC) to 760 HV_{0.1}, which corresponds to the hardness of the hardened base metal ~61 HRC. Lower Vickers hardness values from 710 HV_{0.1} to 610 HV_{0.1} were observed when the samples were hardened at 1150 °C. The highest hardening temperature of 1200 °C and 30% plastic deformation gives the lowest hardness profile HV values, but it decreases from the highest to the lowest (base metal) values, following the same trend (Figure 8).

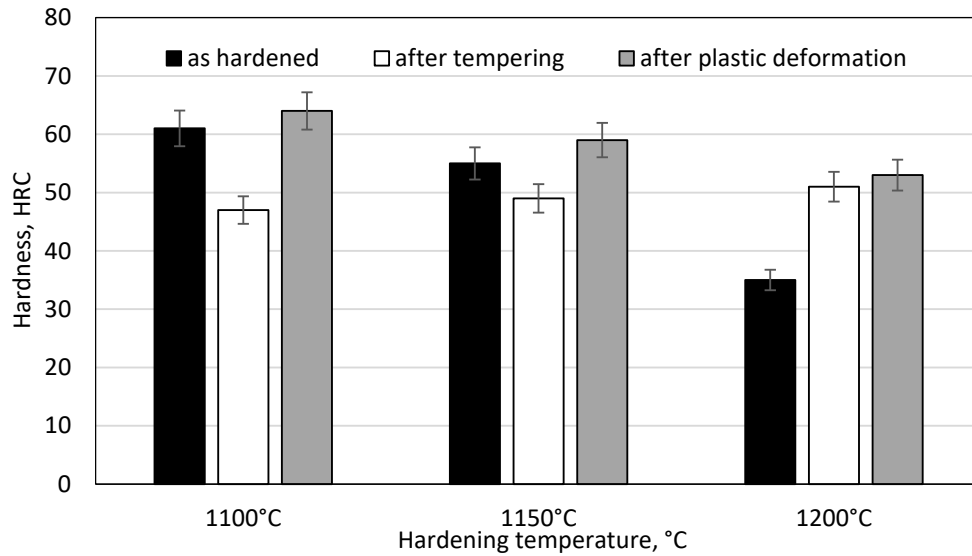


Figure 7. Aggregated hardness values of the samples treated according to the experimental setup.

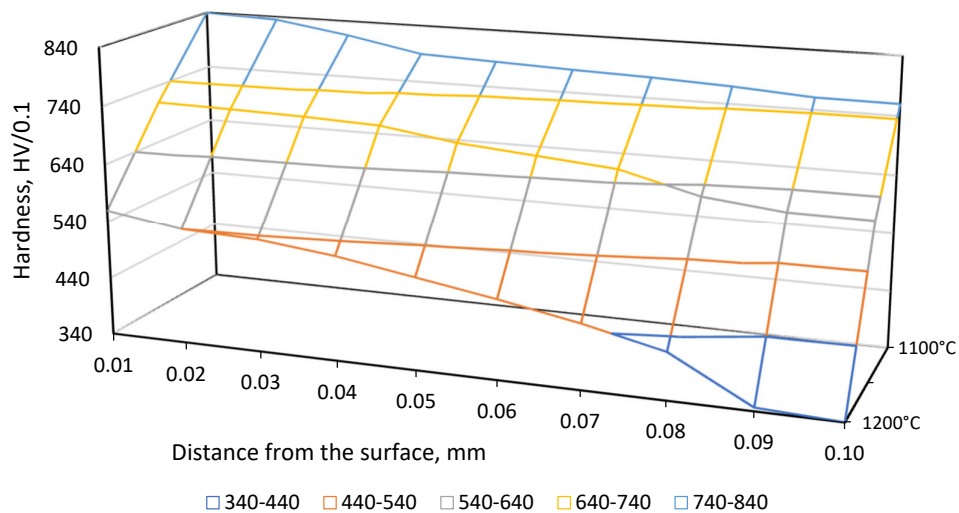


Figure 8. Vickers HV_{0.1} hardness of plastically deformed samples of Batch III.

The positive effect of plastic deformation on the growth of the hardness of the samples is clearly visible. High hardness is a prerequisite for obtaining high wear resistance of cold-worked tool steel, so the ability to obtain high after-hardening hardness is of particular importance [33]. Other authors have noted that wear is strongly dependent on the wear conditions, primarily the speed of the process [14]. They declared that for both speed regimes (sliding speed of 350 and 450 mm/s), the use of lubricant has to be avoided, as it leads to wear drift and an uncontrolled increase in friction coefficient. During plastic deformation, cold work tool steel hardens due to the formation and/or rearrangement of dislocations. Formed martensite acts as a barrier to austenite grain growth and also increases wear resistance [34]. This statement is confirmed by the hardness measurement results (Table 2). Hardness values after all intended tests tended to vary depending on the tempering temperature.

The last and perhaps the most important step of this study was the impact of all research results on wear. Therefore, all samples of all test batches were subjected to an abrasion test. Summarizing the results of the wear experiment, it can be stated that the values of abrasive wear are directly proportional to the results of the previously performed hardness evaluation (Figure 9).

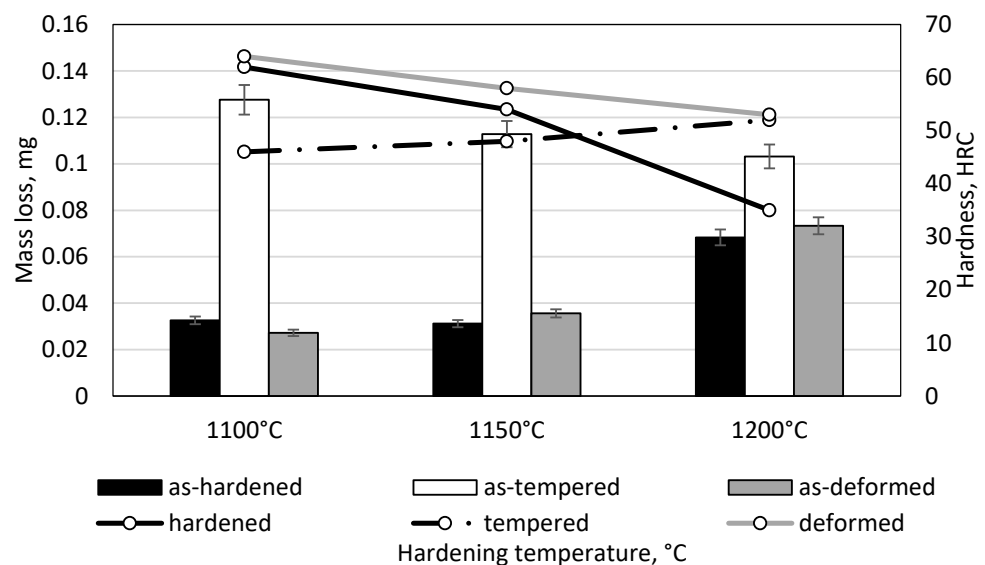


Figure 9. Abrasion and hardness results of the three test batches.

Comparing the hardened and tempered samples, the mass loss of the hardened samples was three to four times lower because their structure was rich in retained austenite, which increases wear resistance. The wear tendency of the deformed layers is very similar to that of the hardened ones; the values change slightly at different tempering temperatures. Plastically deformed samples have finer and more uniformly distributed structures (Figure 6), and as was already reported, they typically exhibit better properties compared to their coarse-grained as-hardened equivalents [18]. Although cold work increases the hardness of metallic materials, which is expected to enhance their wear resistance, the benefits of cold work for wear resistance is lower than that of the as-hardened condition [35]. This could be a direction for further research by changing the amount of plastic deformation or chemical modifications of tool surfaces, such as nitriding [36]. The latter is influenced not only by the nature of the nitrogen, but also by the ability of this substance to diffuse through the steel. Returning to the amount of retained austenite in the as-hardened samples, it is noticeable that the content of residual austenite (~38%) [4] obtained at

the hardening temperature of 1150 °C allowed us to achieve the highest wear resistance of the Batch I samples.

4. Conclusions

1. By increasing the hardening temperature from 1100 °C to 1200 °C, the volume fraction of retained austenite increases from 17.36% to 69.02%, which is more than four times. Retained austenite, identified by bright areas in the microstructure, is significantly more common in the 1200 °C hardened sample than in the samples hardened at lower temperatures such as 1100 °C and 1150 °C.

2. This study shows that increasing the hardening temperature results in a more uniform distribution of carbides, but also requires more thorough tempering to achieve maximum hardness and toughness.

3. In the abrasive wear test, the as-hardened samples lost approximately 3.5 times less mass compared to the tempered ones, indicating a higher wear resistance. Retained austenite increases wear resistance and inhibits crack propagation under abrasive conditions.

4. Plastic deformation after conventional hardening increases the hardness and refines the microstructure of cold work tool steel, resulting in a slight increase in wear resistance compared with as-hardened samples. This highlights the importance of combining heat and mechanical treatments to achieve better properties of cold work tool steels.

5. Overall, the proposed treatment may not be the most economical in terms of energy and time consumption, but if the components' application requires increased wear resistance and longer life, the long-term savings may justify the initial investment.

For future work, exploring alternative deformation methods such as uniform channel angular pressing (ECAP) or high-pressure spinning (HPT) can provide more insight into the optimization of microstructure and wear resistance. Testing other steel grades similar to X160CrMoV12, such as AISI D2, AISI 440C, and AISI 52100, would help generalize these findings. These steels are used in applications that require high hardness and wear resistance, such as in the tool, bearing, and cutting tool industries. To extend this study, testing under different wear conditions such as impact (ASTM G99), fatigue (ASTM G77), or abrasion (ASTM G65) wear would provide a better understanding of material behaviour in various industries where components are exposed to different wear mechanisms. Each of these tests simulates real-world wear scenarios, providing more insight into the durability of steel surfaces under various conditions.

Author Contributions: Conceptualization, R.B.; supervision, R.B.; investigation, R.B.; visualization, R.B.; writing—original draft preparation, R.B.; methodology, L.K.; investigation, L.K.; resources, L.K.; validation, L.K.; writing—reviewing and editing, L.K. All authors have read and agreed to the published version of the manuscript.

Funding: This research did not receive any specific grant from funding agencies in the public, commercial, or not-for-profit sectors.

Data Availability Statement: The original contributions presented in the study are included in the article; further inquiries can be directed to the corresponding author

Conflicts of Interest: The authors declare no conflicts of interest.

References

1. Abdul Rahim, M.A.S.; Minhat, M.; Binti Hussein, N.I.S.; Salleh, M.S. A comprehensive review on cold work of AISI D2 tool steel. *Metall. Res. Technol.* **2018**, *115*, 104. <https://doi.org/10.1051/metal/2017048>.
2. Shasha, Q.; Huan, T.; Hongshan, Z.; Pengfei, H.; Tinghui, T.; Han, D. Microstructural evolution of secondary carbides during spheroidized annealing and quenching and tempering in 60Cr16MoMA martensitic stainless steel. *J. Mater. Res. Technol.* **2024**, *28*, 3207–3219. <https://doi.org/10.1016/j.jmrt.2023.12.264>.
3. Quan, L.; Xiaomi, C.; Kun, L.; Valentino, C.; Lo Kin Ho, A.M.; Zhengchao, X.; Chi Tat, K. Friction stir processing of M2 and D2 tool steels for improving hardness, wear and corrosion resistances. *Surf. Coat. Technol.* **2024**, *481*, 130609. <https://doi.org/10.1016/j.surfcoat.2024.130609>.

4. Kritika, S.; Khatirkar, R.K.; Sapate Sanjay, G. Microstructure evolution and abrasive wear behavior of D2 steel. *Wear* **2015**, 328–329, 206–216. <https://doi.org/10.1016/j.wear.2015.02.019>.
5. Conci, M.D.; Centeno, D.M.A.; Goldenstein, H.; Farina, P.F.S. Study of Short Times Tempering for AISI D2 Cold Work Tool Steel. *Mater. Res.* **2023**, 26, e20230059. <https://doi.org/10.1590/1980-5373-MR-2023-0059>.
6. Trevisiol, C.; Jourani, A.; Bouvier, S. Effect of martensite volume fraction and abrasive particles size on friction and wear behaviour of a low alloy steel. *Trib. Intern.* **2017**, 113, 411–425. <https://doi.org/10.1016/j.triboint.2016.11.001>.
7. Nykiel, T.; Hryniewicz, T. Transformations of Carbides During Tempering of D3 Tool Steel. *J. Mater. Eng. Perform.* **2014**, 23, 2050–2054. <https://doi.org/10.1007/s11665-014-0979-5>.
8. Mochtar, M.A.; Putra, W.N.; Abram, M. Effect of tempering temperature and subzero treatment on microstructures, retained austenite, and hardness of AISI D2 tool steel. *Mater. Res. Express.* **2023**, 10, 13. <https://doi.org/10.1088/2053-1591/acd61b>.
9. Rehan, M.A.; Medvedeva, A.; Svensson, L.E.; Karlsson, L. Retained Austenite Transformation during Heat Treatment of a 5 Wt Pct Cr Cold Work Tool Steel. *Metall. Mater. Transact. A* **2017**, 48A, 5233–5243. <https://doi.org/10.1007/s11661-017-4232-5>.
10. Wong, A. Understanding the Stability of Retained Austenite in High-Carbon Steels. Modelling and Alloy Design. Apollo—University of Cambridge Repository, Cambridge. Ph.D. thesis. 2023. <https://doi.org/10.17863/CAM.96614>.
11. Elhigazi, F.; Artemev, A. The influence of carbide formation in ferrite on the bainitic type transformation. *Comp. Mat. Science.* **2021**, 186, 109961. <https://doi.org/10.1016/j.commatsci.2020.109961>.
12. Adamczyk-Cieslak, B.; Koralnik, M.; Kuziak, R.; Majchrowicz, K.; Zygmunt, T.; Mizera, J. The Impact of Retained Austenite on the Mechanical Properties of Bainitic and Dual Phase Steels. *J. Mater. Eng. Perform.* **2022**, 31, 4419–4433. <https://doi.org/10.1007/s11665-021-06547-w>.
13. Zhirui, W.; Wei, W.; Man, L.; Junyu, T.; Guang, X. Comparison of wear performance of bainitic and martensitic structure with similar fracture toughness and hardness at different wear conditions. *Wear* **2023**, 512–513, 204512. <https://doi.org/10.1016/j.wear.2022.204512>.
14. Boungomba, H.; Moreau, P.; Sadat, T.; Lilosten, L.; Dubar, M.; Dubar, L. Investigation of the impact of AISI D2 tool steel wear and lubrication type on the evolution of the friction coefficient during cold winding process. *Wear* **2024**, 542–543, 205272. <https://doi.org/10.1016/j.wear.2024.205272>.
15. Bendikiene, R.; Kavaliauskiene, L. The effect of plastic deformation rate on the wear performance of hardfaced coatings. *Weld World* **2017**, 61, 893–900. <https://doi.org/10.1007/s40194-017-0476-3>.
16. Lowe, T.C.; Valiev, R.Z. The use of severe plastic deformation techniques in grain refinement. *J. Miner. Met. Mat. Soc.* **2004**, 56, 64–68. <https://doi.org/10.1007/s11837-004-0295-z>.
17. Merah, M.; Azeem, M.A.; Abubaker, H.M.; Al-Badour, F.; Albinmoussa, J.; Sorour, A.A. Friction Stir Processing Influence on Microstructure, Mechanical and Corrosion Behavior of Steels: A Review. *Materials* **2021**, 14, 5023. <https://doi.org/10.3390/ma14175023>.
18. Harish, K.; Kiran, D.; Durgeshwar, P.S.; Jitendra, M.G.; Manish, K.; Vanya, A. Severe plastic deformation: A state of art. *Mater. Today-Proc.* **2023**, 6. <https://doi.org/10.1016/j.matpr.2023.02.194>.
19. Kaveh, E.; Anwar, A.Q.; Saeid, A.; Kei, A.; Aptukov, V.; Asfandiyarov, R.; Maki, A.; Astanin, V.; Bachmaier, A.; Beloshenko, V.; 112 others. Severe plastic deformation for producing Superfunctional ultrafine-grained and heterostructured materials: An interdisciplinary review. *J. Alloys Compd.* **2024**, 1002, 174667. <https://doi.org/10.1016/j.jallcom.2024.174667>.
20. Weidner, A.; Muller, A.; Weiss, A.; Biermann, H. Ultrafine grained high-alloyed austenitic TRIP steel. *Mater. Sci. Eng. A* **2013**, 571, 68–76. <https://doi.org/10.1016/j.msea.2013.02.008>.
21. Seleznev, M.; Mantel, J.; Schmidtchen, M.; Prahl, U.; Biermann, H.; Weidner, A. Steel–Steel Laminates Manufactured via Accumulative Roll Bonding. *Steel Res. Intern.* **2024**, 18, 2400472. <https://doi.org/10.1002/srin.202400472>.
22. Essam, M.A.; Shash, A.Y.; El-Fawakhry, M.K.; El-Kashif, E.; Megahed, H. Effect of Deep Cryogenic Treatment on Wear Behavior of Cold Work Tool Steel. *Metals* **2023**, 13, 382. <https://doi.org/10.3390/met13020382>.
23. Farahany, S.; Ziaie, M.; Nordin, N.A. Effect of Triple Tempering Temperature on Microstructure, Mechanical, and Wear Properties of K340 Cold Work Tool Steel. *J. Mater. Eng. Perform.* **2023**, 32, 9000–9010. <https://doi.org/10.1007/s11665-022-07791-4>.
24. Chi, H.-X.; Ma, D.-S.; Xu, H.-X.; Zhu, W.-L.; Jiang, J.-Q. Phase Transformation of a Cold Work Tool Steel during Tempering. *J. Iron Steel Res. Intern.* **2016**, 23, 484–488. [https://doi.org/10.1016/S1006-706X\(16\)30076-0](https://doi.org/10.1016/S1006-706X(16)30076-0).
25. Bendikiene, R.; Ciuplys, A.; Sertvytis, R.; Surzhenkov, A.; Tkachivskiy, D.; Viljus, M.; Traksmas, R.; Antonov, M.; Kulu, P. Wear behaviour of Cr₃C₂-Ni cermet reinforced hardfacings. *J. Mater. Res. Technol.* **2020**, 9, 7068–7078. <https://doi.org/10.1016/j.jmrt.2020.05.042>.
26. Chandler, H. *Heat Treater's Guide: Practices and Procedures for Irons and Steels*; 2nd edition. ASM International: Metals Park, OH, USA, 1995; p. 904.
27. Kahrobaee, S.; Kashefi, M. Applications of Impedance Plane and Magnetic Differential Permeability in Microstructural Characterization of AISI D2 Tool Steel. *Int. J. Eng.* **2015**, 28, 234–252. <https://doi.org/10.5829/idosi.ije.2015.28.02b.09>.
28. Zheng, Z.; Lei, M.; Huang, C.; Wan, M. Carbide precipitation during tempering of hybrid steel 60. *Mater. Res. Express.* **2024**, 11, 026509. <https://doi.org/10.1088/2053-1591/ad2576>.
29. Günerli, E.; Bayramoğlu, M.; Geren, N. Volume fraction of retained austenite in 1.2842 tool steel as a function of tempering temperature. *Europ. Mech. Sci.* **2022**, 6, 263–268. <https://doi.org/10.26701/ems.1186751>.

30. Liu, B.; Qin, T.; Xu, W.; Ji, C.; Wu, Q.; Chen, M.; Liu, Z. Effect of Tempering Conditions on Secondary Hardening of Carbides and Retained Austenite in Spray-Formed M42 High-Speed Steel. *Materials* **2019**, *12*, 3714. <https://doi.org/10.3390/ma12223714>.
31. Sucupira, F.L.; Sandim, M.J.R.; Sandim, H.R.Z.; Santos Dagoberto, B.; Renzetti, R.A. Quantification of retained austenite by X-ray diffraction and saturation magnetization in a supermartensitic stainless steel. *Mat. Charact.* **2016**, *115*, 90–96. <https://doi.org/10.1016/j.matchar.2016.03.023>.
32. Xingguo, F.; Xiaofeng, X.; Yang, Z.; Dihui, C.; Zhicheng, W.; Xudong, Y.; Yachong, Z.; Yongqiang, Y. Retain the austenite via diffusion control under electropulsing to improve the mechanical properties of the AISI 420 stainless steel. *J. Mater. Res. Technol.* **2024**, *29*, 1665–1674. <https://doi.org/10.1016/j.jmrt.2024.01.177>.
33. Chi, H.; Di, Y.; Zhang, N.; Gu, J.; Zhou, J.; Ma, D. New insight into the relationship between the C-Cr ratio and carbides, mechanical property of cold working die steel. *Mater. Res. Express.* **2023**, *10*, 126512. <https://doi.org/10.1088/2053-1591/ad1545>.
34. Kumar, S.; Maity, S.R.; Patnaik, L. A comparative study on wear behaviors of hot work and cold work tool steel with same hardness under dry sliding tribological test. *Mater. Today Proc.* **2021**, *44*, 949–954. <https://doi.org/10.1016/j.matpr.2020.11.004>.
35. Tang, Y.; Pan, H.; Li, D.Y. Contribution of cold-work to the wear resistance of materials and its limitation—A study combining molecular dynamics modeling and experimental investigation. *Wear* **2021**, *476*, 203642. <https://doi.org/10.1016/j.wear.2021.203642>.
36. Tobola, D.; Brostow, W.; Czechowski, K.; Rusek, P. Improvement of wear resistance of some cold working tool steels. *Wear.* **2017**, *382–383*, 29–39. <https://doi.org/10.1016/j.wear.2017.03.023>.

Disclaimer/Publisher's Note: The statements, opinions and data contained in all publications are solely those of the individual author(s) and contributor(s) and not of MDPI and/or the editor(s). MDPI and/or the editor(s) disclaim responsibility for any injury to people or property resulting from any ideas, methods, instructions or products referred to in the content.